The description and the verification of EAM-potentials at various electron temperatures

Sergei Starikov

The absorption of laser pulse initially leads to the excitation of electron subsystem (ES). In this case initial state of the system is two-temperature (2T) state, and the electron temperature (T_e) may be several orders higher than the ion temperature (T_i). For gold the change of interionic forces plays the key role in dynamics of ions at the initial 2T-stage. One of the ways to describe such process is to use electron-temperature-dependent (ETD) interionic potential in a simulation. Such potential for gold was developed in works [1-3].

For creation of ETD-potential for gold, three EAM-potentials (potentials in the Embedded Atom Method form) at different electron temperatures were created. Construction of the EAM-potentials was performed with force-matching method [4,5]. This technique was used as implemented in the Potfit code [5]. The method provides a way to construct physically justified interparticle potentials without referring to experimental data. The idea is to adjust the interparticle potential to optimally reproduce per-atom forces computed at the *ab initio* level (e.g. with Density Functional Theory) for a fine-tuned set of small reference structures. The reference data were calculated using the VASP code [6]. In our case, the calculations of the reference data were performed at three different T_e (0.1, 3 and 6 eV) that are set as a parameter of the Fermi-Dirac distribution for partial occupancies of electron bands. All the three developed EAM-potentials reproduce forces calculated by the VASP code to within 15–20%, which is quite good accuracy for the given method. The EAM-potential has three independent functions: pair interaction $\varphi(r)$, effective electron density $\rho(r)$ and embedding energy term Φ. Fig. 1 shows the functions of the created EAM-potentials.

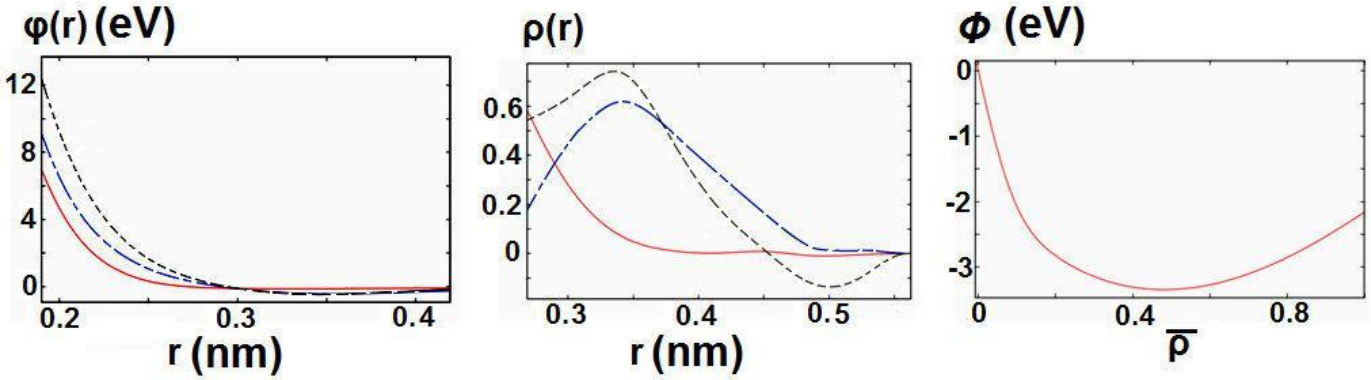

Fig 1. The created EAM-potential functions: $\varphi(r)$ and $\rho(r)$ for gold at various electron temperatures T_e = 0.1 eV (solid curves), 3 eV (dash-dot curves), 6 eV (dashed curves). The "embedding" function Φ(ρ) is shown for T_e = 0.1 eV.

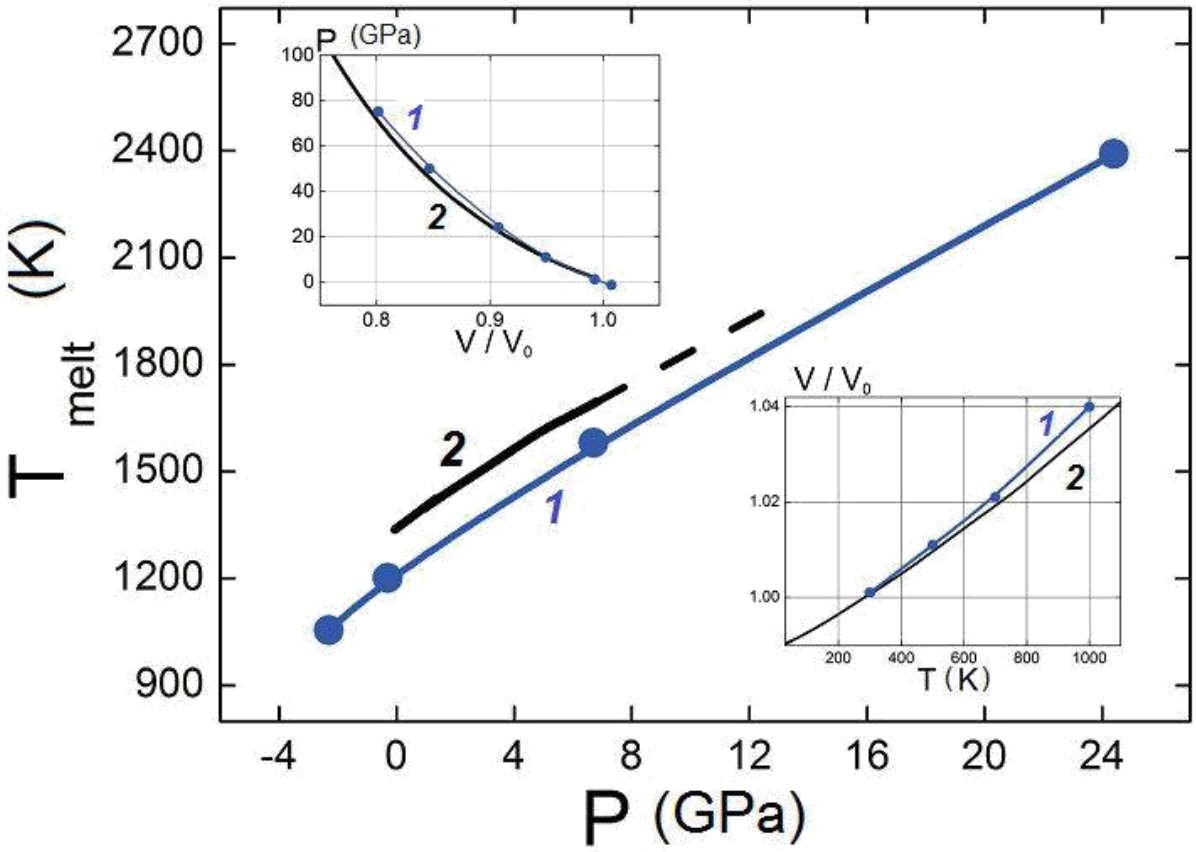

Fig 2. Plots of the melting temperature T_{melt} versus pressure P, room-temperature P versus V isotherm (top inset), and thermal expansion V/V_0 (bottom inset) of gold: (1) simulation using the proposed EAM potential (T_e = 0.1 eV); (2) experimental data [7–9] (V_0 is equilibrium volume)

Fig. 2 and Table show the results of verification of the EAM-potential at T_e = 0.1 eV (*cold part* of ETD-potential). All created EAM-potentials are given in **Au_5T.eam.alloy** file (eam/alloy format for LAMMPS). The indexes **Au**, **Au_3.0**, **Au_6.0** indicate three initially developed EAM-potential: **Au** for EAM-potential at T_e = 0.1 eV (*cold part*), **Au_3.0 Au** for EAM-potential at T_e = 3.0 eV, **Au_6.0 Au** for potential at T_e = 6.0 eV. The indexes **Au_1.5** and **Au_4.5** indicate EAM-potential which were created by interpolation. As the potentials are given in format for alloy, it is necessary to create the cross-pair interactions for various types. All cross-pair interactions are given in **Au_5T.eam.alloy** file as the average pair interactions. For instance the cross pair potential $\varphi(r)$ for "1.5" and "6.0" types is $0.5\cdot(\varphi_{1.5} + \varphi_{6.0})$.

Table. The simulated properties of gold with using of EAM-potential at T_e = 0.1 eV. The experimental data [7–9] are shown in brackets.

V_0 (cm^3 mol^{-1})	E_c (eV)	C_{11} (GPa)	C_{12} (GPa)	T_{melt} (K)
10.23 (10.22)	4.1 (3.8)	230 (202)	180 (170)	1210 (1338)

The properties at high electron temperatures

The ETD-potential may be created using quadratic polynomial interpolation [3]:

$\varphi(r) = \varphi_0 + \varphi_1 T_e + \varphi_2 T_e^2$

and

$\rho(r) = \rho_0 + \rho_1 T_e + \rho_2 T_e^2$.

The ETD-potential coincides with the EAM-potentials at three reference temperatures. At increasing of T_e the ETD-potential may describe the features of 2T-system. In particular, one of the phenomena that can be reproduced by the ETD-potential is an increase of the ion melting temperature T_{melt} at heating of the ES [10]. Fig. 3 shows the results of the simulation.

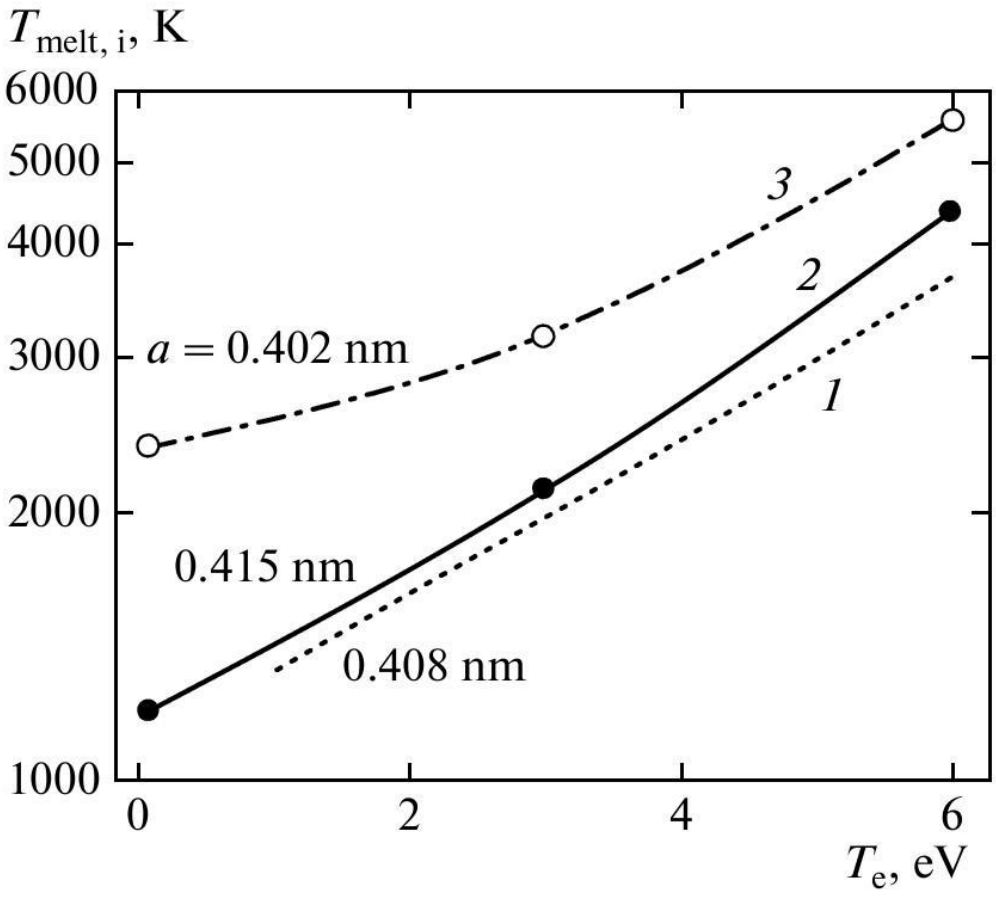

Fig 3. Plots of ion melting temperature T_{melt} versus T_e for gold at various densities (lattice parameters *a*): (1) data from [10]; (2, 3) results of two-phase atomistic simulations in this study for EAM-potentials at T_e = 0.1, 3, and 6 eV.

Another phenomenon that is reproduced by the ETD-potential is increase of the pressure P_e^{loc} of localized electron energy with increase of T_e. In fact, as T_e increases from 0 to 6 eV the pressure in the system described by the ETD-potential increases from 0 to 105 GPa. Together with the value of P_e^{deloc} the total pressure in gold at T_e = 6 eV reaches 200 GPa like in work [10]. Figure 4 shows plots of the total pressure P (*ab initio* calculations using the VASP code) and P_e^{loc} (MD-calculation with the ETD-potential) versus T_e. The difference between the two pressures determines the dependence P_e^{deloc} (T_e).

Some verification of T_e-part of the potentials (about electron pressure) was given in works [11, 12]

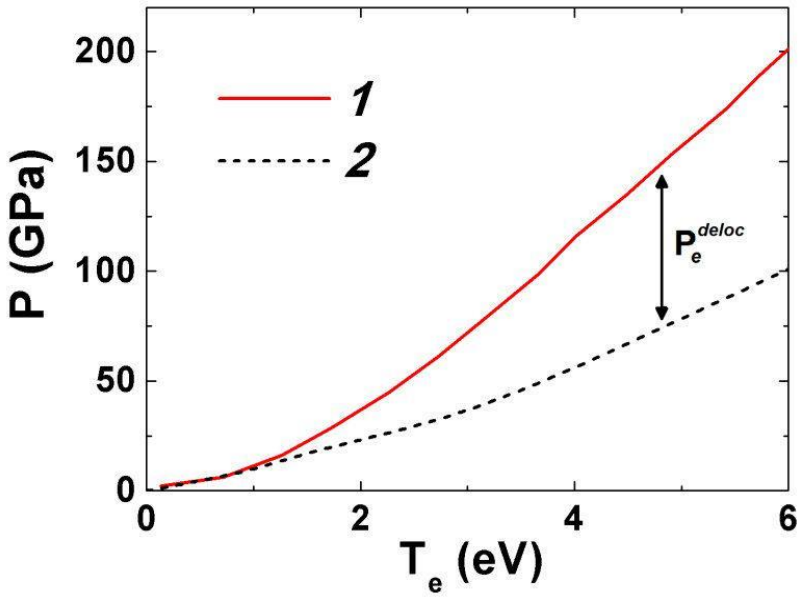

Fig 4. The dependence of pressure on T_e : 1 – total pressure P (*ab initio* calculations with using the VASP code); 2 – the P_e^{loc} reconstructed with the virial theorem (molecular dynamics calculation with the ETD potential). The difference between the two pressures determines the dependence $P_e^{deloc}(T_e)$.

References

[1] G. Norman, S. Starikov, V. Stegailov, V. Fortov, et al., J. Appl. Phys. **112**, 013104 (2012)

[2] G.E. Norman, S.V. Starikov, V.V. Stegailov, Journal of Experimental and Theoretical Physics, **114**, No. 5, pp. 792–800 (2012)

[3] S. Starikov, A. Faenov, T. Pikuz, I. Skobelev, et al., Appl. Phys. B. **116**, P. 1005-1016 (2014)

[4] F. Ercolessi, and J.B. Adams. Europhysics Letters, **26**, 583-588 (1994).

[5] P. Brommer, and F. Gahler. Philosophical Magazine, **86**, 753-758 (2006).

[6] G. Kresse and J. Furthmu¨ller, Phys. Rev. B **54**, 11169–11186 (1996).

[7] J.R. Neighbours, G.A. Alers, Phys. Rev. **111**, P.707 (1958)

[8] P.M. Bell, J. Xu, H.K. Mao, in Shock Waves in Condense Matter, edited by Y.M. Gupta (Plenum, NewYork, 1986).

[9] I.-K. Suh, H. Ohta, Y. Waseda, J. Mater. Sci. **23**, P.757 (1988)

[10] V. Recoules et al. Phys. Rev B, **96**, 05550 (2006)

[11] V. Stegailov and P. Zhilyaev, Pressure in electronically excited warm dense metals, Contrib. Plasma Phys. **55** ,164 – 171 (2015)

[12] V. Stegailov and P. Zhilyaev, Warm dense gold: e ff ective ion–ion interaction and ionization, MOLECULAR PHYSICS (2015)